AIAA JOURNAL
Vol. 34, No. 10, October 1996

Aeroelastic Stability of a Beam Traveling in a Tunnel Lined with Resonators

Nobumasa Sugimoto*
University of Osaka, Toyonaka, Osaka 560, Japan

The theory of aeroelastic wave propagation along a long beam traveling in a tunnel lined with Helmholtz resonators is developed, and the effect of the lining on the stability of the beam is examined. Assuming an elastic beam of uniform cross section and of infinite length, and taking account of the compressibility of the air, the linear dispersion relation is derived for an air-beam-cavity system on disregarding all dissipative effects. The lining newly introduces the cavity mode of propagation in addition to the acoustic mode and the beam mode. When a restoring force in the transverse direction to the beam's axis is present, it is found that all modes are neutrally stable. Without this force, Kelvin–Helmholtz instability occurs in the beam mode for a long wavelength and a low frequency. But the lining does not take part in this instability. The stability of wave propagation is also examined from the standpoint of the wave energy. It is revealed that the cavity mode turns into the mode of so-called negative energy waves as a wave number increases beyond a critical value. Emergence of negative energy waves implies destabilization of the stable modes by weak dissipative effects. The negative energy waves appear also in the beam mode, if the restoring force is absent, in a very narrow band of the wave number.

Nomenclature

a_0 = sound speed in the air
B = throat's cross-sectional area of the Helmholtz resonator
b = radius of the beam
C = complex amplitude of the beam's deflection
$\mathcal{D}$ = dispersion relation
$\mathcal{D}_a, \mathcal{D}_b$ = dispersion relation of the acoustic and beam modes, respectively
E = total wave energy density per unit axial length of the tunnel
EI = flexural rigidity of the beam
$\mathcal{E}$ = temporal average of E over T
F = dimensionless flexural rigidity of the beam
G = dimensionless spring constant
H = deflection of the beam in the y direction as a function of ξ and τ
h = deflection of the beam in the y direction as a function of x and t
J = total wave energy flux density per unit axial length of the tunnel
$\mathcal{J}$ = temporal average of J over T
$\boldsymbol{j}$ = wave energy flux density
K = spring constant of the restoring force per unit axial length of the beam
k = wave number
L = throat's length of the Helmholtz resonator
M = Mach number of the beam's traveling speed, U/a_0
m = beam's mass per unit axial length
m_i = induced mass of the beam
N^* = number density of the resonators per unit area of the tunnel wall including orifices
P = excess pressure in the tunnel over p_0 in the moving frame with the beam
P_c = excess pressure in the cavity over p_0 in the moving frame with the beam
p = excess pressure in the tunnel over p_0 in the frame fixed with the tunnel
p_R = excess pressure at the throat's orifice on the tunnel side
p_c = excess pressure in the cavity of the Helmholtz resonator
p_0 = atmospheric pressure
Q_b = force exerted on the beam by the surrounding air at ξ and τ
q_b = force exerted on the beam by the surrounding air at x and t
R = radius of the tunnel
r = radial coordinate
T = one period of the oscillation in the frame moving with the beam
t = time
U = traveling speed of the beam in the axial direction of the tunnel
V = cavity's volume of the Helmholtz resonator
V^* = N^*V
w = velocity of the air in the throat of the Helmholtz resonator directed into the cavity
w^* = mean velocity of the air averaged over the tunnel wall including orifices
x = axial coordinate along the tunnel
y = transverse coodinate along the deflection of the beam
z = coordinate perpendicular to x and y
β = $(k^2 - \omega^2/a_0^2)^{1/2}$ or $(k^2 - \omega^2)^{1/2}$ in dimensionless form
ε = wave energy density
θ = circumferential angle
κ = smallness of the resonators
ν = ratio of the beam's radius to the tunnel's radius
ξ = axial coordinate in the moving frame with the beam, $x - Ut$
ρ_c = density fluctuation of the air in the cavity of the Helmholtz resonator
ρ_0 = density of the air in equilibrium under the atmospheric
σ = typical induced mass of the beam relative to m
τ = time, t
Φ = velocity potential perturbed from the uniform flow $-U\xi$ in the frame moving with the beam
ϕ = velocity potential in the frame fixed with the tunnel
ω = angular frequency in the frame fixed with the tunnel
ω' = angular frequency in the frame moving with the beam, $\omega - Uk$
ω_0 = natural angular frequency of the Helmholtz resonator

Subscripts

a = air or acoustic mode

Received Nov. 14, 1995; revision received May 20, 1996; accepted for publication May 27, 1996.

*Professor, Department of Mechanical Engineering, Faculty of Engineering Science.

b = beam or beam mode
c = cavity or cavity mode
e = end plane of the control volume
i = inner cylindrical surface of the control volume
l = values at the intersections of two dispersion relations
o = outer cylindrical surface of the control volume

I. Introduction

THIS paper develops the theory of aeroelastic wave propagation to examine the stability of a long beam traveling in a tunnel. Particularly concerned is the effect of the acoustic lining of the tunnel's inner surface with Helmholtz resonators. This problem is motivated by an interest to know how a train behaves aeroelastically when traveling in a tunnel with high speeds and how the lining affects the stability of the train. The lining is proposed for the purpose of inhibiting emergence of an acoustic shock wave in a tunnel generated by a train's entry into the tunnel.[1,2] In fact, the shock wave can occur in long tunnels (of several to 10 km long) for such a low train's Mach number as 0.15. As the train speed is increased, the magnitude of shock wave is strengthened and the shock-formation distance from the tunnel entrance is shortened; namely, the shock wave tends to emerge in shorter tunnels.

To simplify the problem, we assume an elastic beam of uniform cross section and of infinite length. Admittedly, however, this may be insufficient to model an actual train in that it usually comprises many vehicles. To be more realistic, it may be appropriate to assume piecewise uniform beams articulated or coupled simply by pin joints. But since the main concern in this paper is to investigate the effect of the lining, it is the simplest approach to start with the present model. The beam is assumed to be subjected not only to bending but also to a restoring force in the transverse direction to the beam's axis. In a case of magnetically levitated trains, this lateral force is provided by a guideway. Let the inner surface of the tunnel be lined uniformly with the identical Helmholtz resonators. A distance between the neighboring resonators is assumed to be so small compared with a typical wavelength that the effect of the resonators may be smeared out. In general, when a train travels in a tunnel, the surrounding air in an annular region between the train and the tunnel is perturbed and forced into motion by friction. If end effects near the train's head and tail are ignored, the Reynolds number associated with the train speed and its typical diameter takes a very large value on the order of 10^7. Hence turbulence in flows may become important in practice but is ignored here by assuming infinitesimally small disturbances. Furthermore discarding a thermoviscous loss of the air and an intrinsic damping of the beam as well, we derive the linear dispersion relation for aeroelastic wave propagation in the air-beam-cavity system.

But it is not always sufficient to discuss the stability on the basis of the lossless dispersion relation thus derived, even if only the linear theory is concerned. Dissipative effects are always involved more or less. In such a system that there exists an infinitely large store of energy supplied by the traveling of the beam or by the air if viewed from a frame moving with the beam, we cannot say immediately that the dissipative effects lead always to stabilization of neutrally stable waves. In contrast, it often happens that they lead to destabilization. Then the concept of negative energy waves plays an important role in discussing their stability. It was originally conceived by Benjamin[3] and Landahl[4] and later crystallized by Cairns.[5] For some examples, see Ostrovskii et al.[6] and Crighton and Oswell.[7] Whereas usual positive energy waves are stabilized by dissipative effects, negative energy waves are destabilized by them. Intuitively, because any dissipative effects, though assumed to be linear and weak, tend to decrease the wave energy, it follows that the negative energy waves grow in magnitude. To identify the sign of the wave energy, we must establish the energy equation and calculate the average of the wave energy density over one period of oscillation. The sign of the mean wave energy density can then be derived from the lossless dispersion relation.

In the following, the formulation of the problem is first given in Sec. II and the linear dispersion relation is then derived in Sec. III. Section IV is devoted to numerical evaluation of the dispersion relation and also to its asymptotic evaluation in the case of weak aeroelastic coulping. In Sec. V, the mean wave energy is shown to be derived from the dispersion relation and the mode of the negative energy waves is identified.

II. Formulation of the Problem

We start with formulating the problem. Suppose an infinitely long tunnel of radius R. Take the (x, y, z) Cartesian coordinate system and the (r, θ, x) cylindrical coordinate system so that the x axis may be taken in common along the center axis of the tunnel. The cross-sectional configuration is shown in Fig. 1. An elastic beam of radius $b(<R)$ extends to infinity along its axis, and it travels with a constant speed in the x direction. This speed is smaller, of course, than the sound speed in the surrounding air. In the unperturbed state, the beam is straight and concentric with the tunnel, whereas the quiescent air fills the annular region $b < r < R$ and the resonators through orifices. All dissipative effects and the gravity are ignored.

When the beam is bent because of air–beam interaction, it is constrained to deflect in the y direction only and is subjected to the restoring force proportional to the deflection. The inner surface of the tunnel is lined uniformly with many but identical resonators and is smooth and rigid. Since the distance between the neighboring resonators is taken to be small enough compared with a typical wavelength, the resonators are regarded as being distributed continuously and their effect is considered in the averaged form over the inner surface of the tunnel including the throat's orifices.

On assuming infinitesimal deflection of the beam, the behavior of the perturbed air is described on taking account of its compressibility by the following equation for $\phi(r, \theta, x, t)$:

$$\frac{\partial^2\phi}{\partial t^2} = a_0^2\left(\frac{\partial^2\phi}{\partial r^2} + \frac{1}{r}\frac{\partial\phi}{\partial r} + \frac{1}{r^2}\frac{\partial^2\phi}{\partial\theta^2} + \frac{\partial^2\phi}{\partial x^2}\right) \tag{1}$$

In terms of ϕ, the excess pressure p is given by

$$p(r, \theta, x, t) = -\rho_0\frac{\partial\phi}{\partial t} \tag{2}$$

and the density fluctuation is given by p/a_0^2.

When the beam is deflected by $h(x, t)$, the kinematical boundary condition at the beam's surface requires that

$$\frac{\partial\phi}{\partial r} = \frac{\partial h}{\partial t}\cos\theta \qquad \text{at} \qquad r = b \tag{3}$$

As the beam is moving in the axial direction, it is appropriate to take the moving frame ξ and τ instead of x and t. In this frame, the flexural motion of the beam is governed by

$$m\frac{\partial^2 H}{\partial\tau^2} + EI\frac{\partial^4 H}{\partial\xi^4} + KH = Q_b \tag{4}$$

for $H(\xi, \tau)[=h(\xi + U\tau, \tau)]$. Here Q_b is calculated as follows. The force q_b acting on the beam at x in the fixed frame is given by

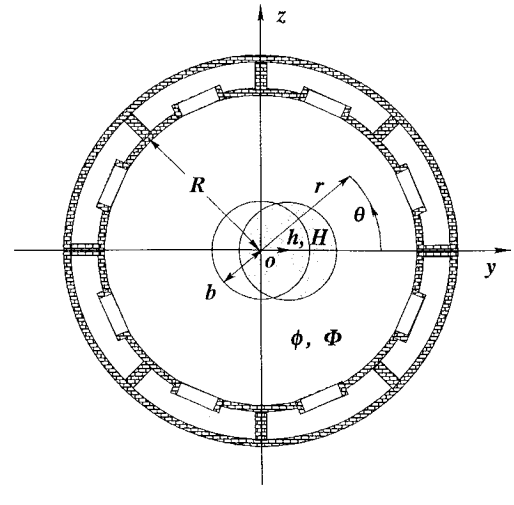

Fig. 1 Cross-sectional configuration of a tunnel lined acoustically with Helmholtz resonators.

integrating the pressure over the beam's surface per unit axial length as

$$q_b(x,t) = \rho_0 b \int_0^{2\pi} \left.\frac{\partial \phi}{\partial t}\right|_{r=b} \cos\theta \, d\theta \tag{5}$$

Because the beam is moving, $Q_b(\xi, \tau)$ is given by $q_b(\xi + U\tau, \tau)$.

Next we formulate the resonator's response to the external pressure fluctuation at its orifice.[1] Assuming that the cavity's volume is much larger than the throat's, the motion of the air in the cavity is ignored so that only the mass conservation is concerned:

$$V\frac{\partial \rho_c}{\partial t} = \rho_0 B w \tag{6}$$

Because the throat's length is much shorter than a typical wavelength, the air in the throat may be regarded as being incompressible and is driven by the pressure difference between p_c and p_R. The equation of motion for the air in the throat is then given by

$$\rho_0 L\frac{\partial w}{\partial t} = -p_c + p_R \tag{7}$$

where w is assumed uniform along the throat. Eliminating w in Eqs. (6) and (7), we derive a single equation for p_c by using $p_c = a_0^2 \rho_c$:

$$\frac{\partial^2 p_c}{\partial t^2} + \omega_0^2 p_c = \omega_0^2 p_R \tag{8}$$

where ω_0 is given by $(Ba_0^2/LV)^{1/2}$. With p_R given by $p(R, \theta, x, t)$, p_c, ρ_c, and w are functions of θ and x as well as t.

Since the tunnel wall is assumed to be smooth and rigid, the velocity component normal to it must vanish there. The velocity component normal to the inner surface of the tunnel is averaged over the unit area of the surface and its mean velocity is given by

$$w^*(\theta, x, t) = N^* B w = \frac{V^*}{\rho_0 a_0^2}\frac{\partial p_c}{\partial t} \tag{9}$$

Hence the boundary condition at the inner surface of the tunnel is taken as

$$\frac{\partial \phi}{\partial r} = w^* \qquad \text{at} \qquad r = R \tag{10}$$

III. Dispersion Relation

Let us now derive the dispersion relation of wave propagation by assuming sinusoidal deflection of the beam in the form of

$$h(x,t) = C\exp[i(kx - \omega t)] \tag{11}$$

where k is taken to be real, whereas ω is complex in general, as will be determined by the dispersion relation. In the moving frame, Eq. (11) is given by

$$H(\xi, \tau) = C\exp[i(k\xi - \omega' t)] \tag{12}$$

In view of Eqs. (11) and (3), a solution to Eq. (1), ϕ, is sought in the following form:

$$\phi = f(r)\cos\theta \exp[i(kx - \omega t)] \tag{13}$$

Then the boundary condition (3) is imposed on f as

$$\frac{df}{dr} = -i\omega C \qquad \text{at} \qquad r = b \tag{14}$$

Expressing p_R in terms of f and using Eq. (8), it follows that

$$p_c = \frac{i\rho_0\omega}{1 - \omega^2/\omega_0^2} f(R)\cos\theta \exp[i(kx - \omega t)] \tag{15}$$

Further using Eq. (9), the boundary condition (10) is given by

$$\frac{df}{dr} = \frac{V^*}{a_0^2}\frac{\omega^2}{(1 - \omega^2/\omega_0^2)} f(R) \qquad \text{at} \qquad r = R \tag{16}$$

Substituting Eq. (13) into Eq. (1), one sees that $f(r)$ satisfies Bessel's equation:

$$\frac{d^2 f}{dr^2} + \frac{1}{r}\frac{df}{dr} - \left(\beta^2 + \frac{1}{r^2}\right) f = 0 \tag{17}$$

with $\beta^2 = k^2 - \omega^2/a_0^2$. This equation is solved in terms of the modified Bessel functions I_1 and K_1 of the first order as follows:

$$f(r) = C_1 I_1(\beta r) + C_2 K_1(\beta r) \tag{18}$$

where C_1 and C_2 are as yet arbitrary constants to be determined by the boundary conditions (14) and (16). To simplify their resultant expressions, it is convenient to introduce D_j $(j = 1, 2, 3, 4)$ defined, respectively, by

$$\begin{aligned} D_1 &= I_1(\beta b)K_1(\beta R) - K_1(\beta b)I_1(\beta R) \\ D_2 &= I_1'(\beta b)K_1(\beta R) - K_1'(\beta b)I_1(\beta R) \\ D_3 &= I_1(\beta b)K_1'(\beta R) - K_1(\beta b)I_1'(\beta R) \\ D_4 &= I_1'(\beta b)K_1'(\beta R) - K_1'(\beta b)I_1'(\beta R) \end{aligned} \tag{19}$$

where the prime implies differentiation with respect to the argument. Note that the logarithmic singularity involved in K_1 cancels out in D_j $(j = 1, 2, 3, 4)$ and that D_1 and D_4 are even functions of β, whereas D_2 and D_3 are odd in a sense that they do not change or change sign by replacement of β with $-\beta$. Furthermore we can prove that there exists a simple relation among D_j $(j = 1, 2, 3, 4)$ that

$$D_1 D_4 - D_2 D_3 = 1/bR\beta^2 \tag{20}$$

which will be used later.

Setting $\mathcal{F}_1$ and $\mathcal{F}_2$ to be

$$\mathcal{F}_1 = \beta D_3 - \frac{V^*}{a_0^2}\frac{\omega^2}{(1 - \omega^2/\omega_0^2)} D_1 \tag{21}$$

$$\mathcal{F}_2 = \beta^2 D_4 - \frac{V^*}{a_0^2}\frac{\omega^2}{(1 - \omega^2/\omega_0^2)} \beta D_2 \tag{22}$$

C_1 and C_2 are determined in terms of C as follows:

$$C_1 = -\frac{i\omega}{\mathcal{F}_2}\left[\beta K_1'(\beta R) - \frac{V^*}{a_0^2}\frac{\omega^2}{(1 - \omega^2/\omega_0^2)} K_1(\beta R)\right] C \tag{23}$$

$$C_2 = \frac{i\omega}{\mathcal{F}_2}\left[\beta I_1'(\beta R) - \frac{V^*}{a_0^2}\frac{\omega^2}{(1 - \omega^2/\omega_0^2)} I_1(\beta R)\right] C \tag{24}$$

With C_1 and C_2 thus specified, $f(R)$, p_R, and p_c are expressed as follows:

$$f(R) = (i\omega/R\mathcal{F}_2)C \tag{25}$$

$$p_R = -(\rho_0\omega^2/R\mathcal{F}_2)C\cos\theta\exp[i(kx - \omega t)] \tag{26}$$

$$p_c = -\frac{\rho_0\omega^2}{R\mathcal{F}_2(1 - \omega^2/\omega_0^2)} C\cos\theta\exp[i(kx - \omega t)] \tag{27}$$

Having obtained the flowfield with C given, the force acting on the beam is calculated by using Eq. (5). In the moving frame, it is given by

$$Q_b = -i\pi\rho_0 b\omega f(b)\exp[i(k\xi - \omega'\tau)] \tag{28}$$

with

$$f(b) = -i\omega(\mathcal{F}_1/\mathcal{F}_2)C \tag{29}$$

Upon substituting Eqs. (12) and (28) with Eq. (29) in Eq. (4), it is required for C to be nontrivial that

$$Y - \pi\rho_0 b\omega^2(\mathcal{F}_1/\mathcal{F}_2) \equiv \mathcal{D} = 0 \tag{30}$$

where $Y = m\omega'^2 - EIk^4 - K$. Replacing β involved in $\mathcal{F}_1$ and $\mathcal{F}_2$ with $(k^2 - \omega^2/a_0^2)^{1/2}$, we derive the desired dispersion relation between k and ω (or ω').

IV. Wave Propagation and Stability

A. Numerical Evaluation

We now examine the dispersion relation and discuss the stability of wave propagation. First, it is appropriate to rewrite Eq. (30) in a dimensionless form. The wave number and the angular frequency are normalized, respectively, by setting

$$kR \to k \qquad \text{and} \qquad \omega R/a_0 \to \omega \tag{31}$$

while the following dimensionless parameters are introduced:

$$\frac{b}{R} \equiv \nu(<1), \qquad \frac{U}{a_0} \equiv M(<1), \qquad \frac{\pi\rho_0 b^2}{m} \equiv \sigma$$
$$\frac{EI}{mR^2a_0^2} \equiv F, \qquad \frac{KR^2}{ma_0^2} \equiv G, \qquad \frac{2V^*}{R} \equiv \kappa \tag{32}$$

In accordance with this normalization, the arguments of D_j $(j = 1, 2, 3, 4)$ in Eq. (19) should be understood as $\beta b \to \beta\nu$ and $\beta R \to \beta$ with $\beta^2 = k^2 - \omega^2$ in the dimensionless form. Furthermore, setting $\omega_0 R/a_0 \to \omega_0$, one can rewrite Eq. (30) after a little manipulation as

$$[(\omega - Mk)^2 - Fk^4 - G]$$
$$\times \left[\left(1 - \omega^2/\omega_0^2\right)\beta^2 D_4 - (\kappa/2)\omega^2\beta D_2\right]$$
$$= (\sigma/\nu)\left[\left(1 - \omega^2/\omega_0^2\right)\beta D_3 - (\kappa/2)\omega^2 D_1\right]\omega^2 \tag{33}$$

where σ designates the ratio of a typical induced mass of the cylindrical beam to the actual mass per unit axial length and controls the degree of aeroelastic coupling. In fact, $\pi\rho_0 b^2$ is the induced mass of the cylinder in the limits of a low frequency $\omega \to 0$ and of a thin beam $\nu \to 0$. For an arbitrary frequency, the induced mass depends on the frequency and also geometrical configuration (see Appendix A). The ratio σ is very small, as expected. If σ is ignored, Eq. (33) is decoupled into two factors for independent modes of propagation. The first factor represents the dispersion relation of the flexural waves propagating on the beam. This is called the beam mode. The second factor represents that of the acoustic waves propagating in the annular region when the beam is free from deflection (i.e., $C \equiv 0$). This is called the acoustic mode. Note that this mode has $\cos\theta$ dependence and is nonaxisymmetric. When the tunnel is not lined, i.e., $\kappa = 0$, the dispersion relation of the acoustic mode is given simply by $k^2 - \omega^2 = \zeta_n^2$ where ζ_n $(n = 1, 2, 3, \ldots)$ are the roots of D_4 and ζ_n are pure imaginary and nonzero because $\beta^2 D_4$ approaches $(1 - \nu^2)/(2\nu^2)$ as $\beta \to 0$ [see Eq. (35)]. Then the root of $1 - \omega^2/\omega_0^2 = 0$ is spurious. But when κ is present, there appears another mode of propagation from this spurious root. This is the cavity mode associated with the lining and is distinguished from the acoustic mode associated with the roots of D_4. Incidentally, the factor in the square brackets on the right-hand side of Eq. (33) is the dispersion relation in a case that the boundary condition (14) at $r = b$ is replaced by $p = 0$, i.e., $f(b) = 0$.

To evaluate the dispersion relation numerically, we employ the following plausible values:

$$b = 1.5\,\text{m}, \qquad R = 5\,\text{m}, \qquad \rho_0 = 1.2\,\text{kg/m}^3$$
$$a_0 = 340\,\text{m/s}, \qquad m = 2.4 \times 10^3\,\text{kg/m} \tag{34}$$
$$EI = 2 \times 10^9\,\text{kgm}^3/\text{s}^2$$

so that $\nu = 0.3$, $\sigma = 3.5 \times 10^{-3}$, and $F = 0.29$. The preceding data will not differ significantly from those to be used in actual cases. But a choice of G and κ is determined by the design of the train–tunnel system. In G, K/m determines a typical frequency of oscillation in the transverse direction of the beam. If this frequency is designed to be as low as 2π rad/s (1 Hz), G is found to take a small value of 8.5×10^{-3}. On the other hand, κ measures the smallness of the resonators. This represents the ratio of the total volume of the resonators per unit axial length of the tunnel, $2\pi RN^*V$, to the tunnel's cross-sectional area πR^2. The value of κ is usually taken to be much smaller than unity, e.g., 0.1.

We first examine the dispersion relation in the limit of a long wavelength $k \to 0$ and a low frequency $\omega \to 0$. As β^2 is correspondingly small, D_j $(j = 1, 2, 3, 4)$ in Eq. (19) are expanded in terms of β after normalization. It then follows that

$$D_1 = -\frac{1 - \nu^2}{2\nu} + \mathcal{O}(\beta^2), \qquad D_2 = \frac{1 + \nu^2}{2\nu^2\beta} + \mathcal{O}(\beta)$$
$$D_3 = -\frac{1 + \nu^2}{2\nu\beta} + \mathcal{O}(\beta), \qquad D_4 = \frac{1 - \nu^2}{2\nu^2\beta^2} + \mathcal{O}(1) \tag{35}$$

Approximating D_j $(j = 1, 2, 3, 4)$ in Eq. (33) by Eq. (35) and assuming G to be small and comparable with k^2, k, and ω satisfy the following equation to the lowest approximation:

$$(1 + \sigma s)\omega^2 - 2M\omega k + (M^2k^2 - G) = 0 \tag{36}$$

with $s = (1 + \nu^2)/(1 - \nu^2)$. In the limit of a long wavelength, ω approaches a finite value

$$\omega = \pm[G/(1 + \sigma s)]^{\frac{1}{2}} \equiv \pm\omega_G \tag{37}$$

If G vanishes, then ω is given by

$$\omega = \left[\frac{1 \pm i(\sigma s)^{\frac{1}{2}}}{1 + \sigma s}\right]Mk \tag{38}$$

This implies temporal instability as well as damping. Such an instability may be classified as the class C instability or Kelvin–Helmholtz instability of Benjamin. From a detailed analysis, it is found that this instability occurs for a wave number in an interval $0 < k < k_f$ with $k_f = (\sigma s/F)^{1/2}M + \mathcal{O}(\sigma^{3/2})$. Given $\sigma s/F$, k_f increases in proportion to the Mach number M. It also increases as the beam becomes lighter or less rigid. But the resonators do not take part in this instability.

We now demonstrate the dispersion relation by solving Eq. (33) numerically. First we consider a case of an ordinary tunnel by setting $\kappa = 0$. Figure 2 shows the dispersion curves for $M = 0.4$ and $G = 0.01$. There exists no imaginary part in ω. The dispersion curves of Eq. (33) are symmetric with respect to the origin $k = \omega = 0$, and therefore the half-plane $k > 0$ is shown. A unit wave number and a unit angular frequency correspond, respectively, to a wavelength of 31.4 m and a frequency of 10.8 Hz. Over the range $0 \le k \le 5$ and $-5 \le \omega \le 5$, there appear four branches where the dotted line corresponds to the line $\omega = Mk$. The sign attached to the curves indicates that of $\partial\mathcal{D}/\partial\omega$, whose physical meaning will be explained later.

The dispersion curves appear to cross but do not touch each other. Because the right-hand side of Eq. (33) is very small, they are substantially the acoustic mode or the beam mode in the case with $\sigma = 0$. For a small value of σ, however, they are bent sharply to avoid crossing. There each curve cannot be identified clearly as the

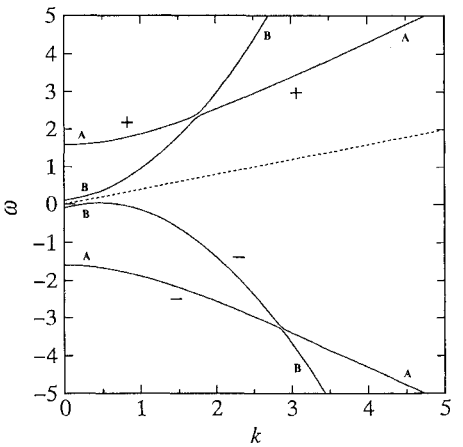

Fig. 2 Dispersion relation in the case with the lateral restoring force $G = 0.01$ but without the lining $\kappa = 0$ for $M = 0.4$, where A and B stand for the acoustic and beam modes, respectively, with the sign of $\partial\mathcal{D}/\partial\omega$, and the dotted line represents the line $\omega = Mk$.

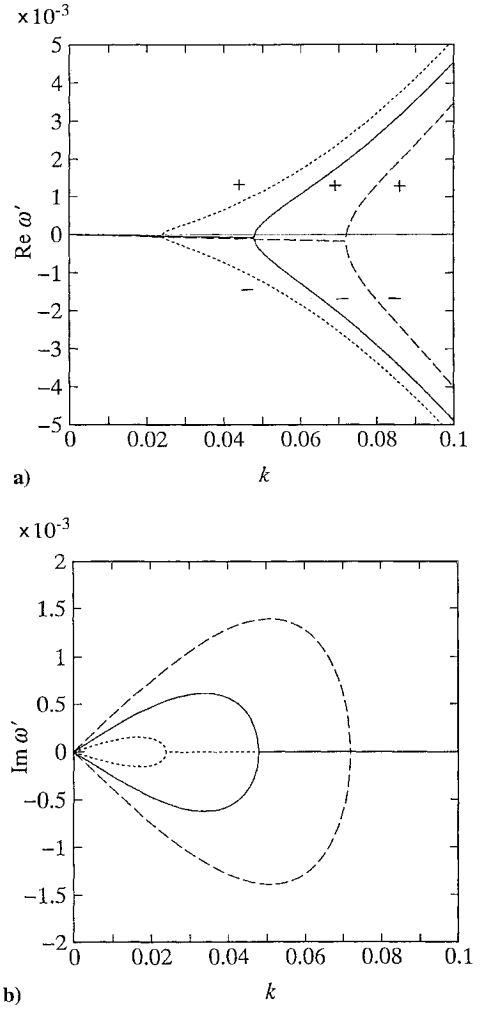

Fig. 3 Dispersion relation between k and ω' ($= \omega - Mk$) for the beam mode in the case without the lateral restoring force and the lining, i.e., $G = \kappa = 0$ for three values of M: a) and b) display the real and imaginary parts of ω', respectively, where the dotted, solid, and broken lines represents the cases with $M = 0.2, 0.4$, and 0.6, respectively, and the sign in a) indicates that of $\partial\mathcal{D}/\partial\omega$ for $k > k_f$.

acoustic mode or the beam mode. In fact, the curve starting from $\omega \approx 0.09979$ at $k = 0$ by Eq. (37) is the beam mode but is bent sharply to approach the acoustic mode as $k \to \infty$. Another curve starting from $\omega \approx 1.584$ at $k = 0$ is the acoustic mode but bent to approach the beam mode as $k \to \infty$. For the remaining curves, the same holds. But we still call the curves except in the vicinity of the intersections according to the names for the independent modes of propagation in the case with $\sigma = 0$.

If G vanishes, the imaginary part appears in the beam mode near the origin. Figure 3 displays the real and imaginary parts of $\omega'(= \omega - Mk)$ against k for $\kappa = 0$ and three values of M where the dotted, solid, and broken lines correspond, respectively, to the case with $M = 0.2, 0.4$, and 0.6. For $k < k_f$, the imaginary part of ω appears in the form of the complex conjugate pair. As k increases beyond k_f, the imaginary part vanishes and the real part bifurcates into two branches. Hence the instability occurs for $k < k_f$. Then the beam is destabilized by the ambient air. But the wavelength corresponding to k_f is found to be very long, about 450 m even for $M = 0.6$. Except in the vicinity of the origin as shown in Fig. 3, the qualitative features of the dispersion curves are similar to those in Fig. 2. As k increases, in fact, the upper and lower branches in Fig. 3a approach, respectively, the curves in Fig. 2 starting from $\omega = \omega_G$ and $-\omega_G$ at $k = 0$.

Next we examine the effect of the resonators. Figure 4 shows the dispersion relation for $M = 0.4, G = 0.01, \kappa = 0.1$, and $\omega_0 = 1.25$ where the other parameters are fixed and the dotted line corresponds to the line $\omega = Mk$. A remarkable difference from Fig. 2 is that

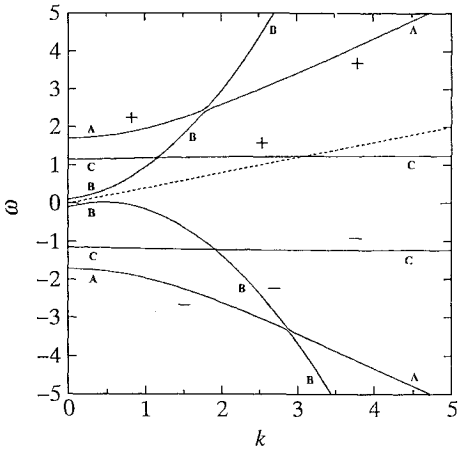

Fig. 4 Dispersion relation in the case with the lateral restoring force and the lining with the resonators, $G = 0.01$, $\kappa = 0.1$, and $\omega_0 = 1.25$, for $M = 0.4$, where A, B, and C stand for the acoustic, beam, and cavity modes, respectively, with the sign of $\partial\mathcal{D}/\partial\omega$, and the dotted line represents the line $\omega = Mk$.

there appear two more branches almost parallel to the k axis. They represent the cavity mode. The curve starting from $\omega \approx 0.09979$ at $k = 0$ is the beam mode. But it is bent horizontally around $k = 1.2$ to approach the cavity mode as $k \to \infty$ with $\omega \to \omega_0 = 1.25$. Another curve starting from $\omega \approx 1.1450$ at $k = 0$ is the cavity mode. As k increases, it is first bent to coincide with the beam mode for a while and bent again to approach the acoustic mode as $k \to \infty$. In this figure as well, all branches neither cross each other nor have the imaginary part. Hence all modes are neutrally stable. If we consider the case with $\kappa = 0.1$ but with $G = 0$ to examine the effect of resonators on the instability of the beam mode as shown in Fig. 3, the curves are little affected. Thus as far as the lossless dispersion relation is concerned, the resonators do not play a primary role in the instability of the beam mode near the origin for the present choice of the parameters.

B. Asymptotic Evaluation

In the preceding subsection, the dispersion relation has been evaluated numerically for the plausible values of the parameters. In view of the results, we examine it asymptotically by exploiting the fact that σ is usually very small. In addition, the smallness of κ may also be exploited for further simplification. When σ is neglected in Eq. (33), we have two independent dispersion relations factorized on the left-hand side:

$$(\omega - Mk)^2 - Fk^4 - G \equiv \mathcal{D}_b(k, \omega) = 0 \tag{39}$$

and

$$\left(1 - \omega^2/\omega_0^2\right)\beta^2 D_4 - (\kappa/2)\omega^2\beta D_2 \equiv \mathcal{D}_a(k, \omega) = 0 \tag{40}$$

But this approximation becomes invalid in the vicinity of the intersections of two curves of Eqs. (39) and (40) in the (k, ω) plane because the right-hand side of Eq. (33) no longer remains small in comparison with the left-hand side. This case should be treated separately.

Let the intersections be denoted by $k = k_l$ and $\omega = \omega_l$ ($l = \pm 1, \pm 2, \pm 3, \ldots$), where $\mathcal{D}_b(k_l, \omega_l) = \mathcal{D}_a(k_l, \omega_l) = 0$. The positive or negative suffixes l represent the intersections located in the upper or lower plane of ω, respectively. The intersections are ordered from the smallest in magnitude of the frequencies and numbered $l = 1, 2, 3, \ldots$ in the upper plane and $l = -1, -2, -3, \ldots$ in the lower plane, respectively. Note that ω_0 is the natural frequency of the resonator. Setting $\delta k = k - k_l$ and $\delta\omega = \omega - \omega_l$, $\mathcal{D}_b$ and $\mathcal{D}_a$ are expanded about k_l and ω_l up to the first order of δk and $\delta\omega$. Here δk and $\delta\omega$ are assumed to be small of order $\sigma^{1/2}$. It then follows from Eq. (33) to the lowest order of σ that

$$\alpha_l(\delta\omega - V_{bl}\delta k)(\delta\omega - V_{al}\delta k) + \mu_l = 0 \tag{41}$$

with

$$\alpha_l = \left.\frac{\partial \mathcal{D}_b}{\partial \omega}\right|_l \left.\frac{\partial \mathcal{D}_a}{\partial \omega}\right|_l \tag{42}$$

$$V_{bl} = -\left.\frac{\partial \mathcal{D}_b/\partial k}{\partial \mathcal{D}_b/\partial \omega}\right|_l, \qquad V_{al} = -\left.\frac{\partial \mathcal{D}_a/\partial k}{\partial \mathcal{D}_a/\partial \omega}\right|_l \tag{43}$$

and

$$\mu_l = -(\sigma/\nu)\left\{\left[1 - \left(\omega_l^2/\omega_0^2\right)\right]\beta_l D_3 - (\kappa/2)\omega_l^2 D_1\right\}\omega_l^2 \tag{44}$$

where $\ldots|_l$ implies the quantity evaluated at k_l and ω_l; V_{bl} and V_{al} denote the group velocity determined by Eqs. (39) and (40) at the intersection, respectively; β in D_j $(j = 1, 2, 3, 4)$ is understood as $(k_l^2 - \omega_l^2)^{1/2} = \beta_l$. Making use of Eqs. (40) and (20), μ_l is rewritten as

$$\mu_l = \frac{\sigma\left(1 - \omega_l^2/\omega_0^2\right)\omega_l^2}{\nu^2 \beta_l D_2} \tag{45}$$

Thus the dispersion relation in the vicinity of the intersection is approximated by the quadratic relation (41).

When Eq. (41) is solved for $\delta\omega$ in terms of a real δk, there are two cases; i.e., $\delta\omega$ is real or complex. The former corresponds to the case of the numerical result in the preceding subsection. In the latter case, it is classified as Kelvin–Helmholtz instability. This case is possible if the following inequality holds:

$$(V_{bl} - V_{al})^2(\delta k)^2 - (4\mu_l/\alpha_l) < 0 \tag{46}$$

If μ_l/α_l is positive, $\delta\omega$ becomes complex for the wave number in the band $|\delta k| < [4\mu_l/\alpha_l(V_{bl} - V_{al})^2]^{1/2}$. Thus the sign of μ_l/α_l determines the instability.

At first, we consider μ_l/α_l at the intersections between the acoustic mode and the beam mode. Since κ is small, β_l is close to one of the ζ_n $(n = 1, 2, 3, \ldots)$, say ζ_l. Then the derivative of $\mathcal{D}_a$ with respect to ω may be approximated, neglecting the terms of order κ, to be

$$\left.\frac{\partial \mathcal{D}_a}{\partial \omega}\right|_l \approx -\left(1 - \frac{\omega_l^2}{\omega_0^2}\right)\frac{\omega_l}{\beta_l}\frac{\mathrm{d}}{\mathrm{d}\beta}\left(\beta^2 D_4\right) \tag{47}$$

By making use of the relations

$$\frac{\mathrm{d}}{\mathrm{d}\beta}\left(\beta^2 D_4\right) = \beta\left[\left(\beta + \frac{1}{\beta}\right)D_2 + \left(\nu\beta + \frac{1}{\nu\beta}\right)D_3\right] \tag{48}$$

and $\partial \mathcal{D}_b/\partial\omega|_l = 2(\omega_l - Mk_l) = 2\omega_l'$, we can evaluate μ_l/α_l for a small value of κ approximately by

$$\frac{\mu_l}{\alpha_l} \approx -\frac{\sigma\omega_l}{2\nu^2\omega_l'}\left[\left(\beta_l^2 + 1\right)D_2^2 + \left(\nu\beta_l^2 + \frac{1}{\nu}\right)D_2 D_3\right]^{-1} \tag{49}$$

where β_l is replaced by ζ_l.

According to Eq. (49), we check the sign of μ_l/α_l at the intersections between the lowest acoustic mode and the beam mode. In the case of Fig. 4, these intersections are represented by the suffix $l = \pm 2$. In the case with $\sigma = 0$ for $\nu = 0.3$, we have $k_2 = 1.790$, $\omega_2 = 2.444$ for $l = 2$ so that $\beta_2 = 1.663i$. If the effect of κ is ignored, $\zeta_2 = 1.582i$, $D_2 = -2.719i$, and $D_3 = 0.4897i$, where the relative error $|(\beta_2 - \zeta_2)/\beta_2|$ is about 5%, which is within the order of κ. Thus it follows that μ_l/α_l takes the negative sign so that no instability occurs.

Next we examine the case of the intersections between the cavity mode and the beam mode. In this case, μ_l in Eq. (45) can alternatively be written as

$$\mu_l = \frac{\sigma\kappa\omega_l^4}{2\nu^2\beta_l^2 D_4} \tag{50}$$

For a small value of κ, ω_l is nearly equal to $\pm\omega_0$ and $\partial \mathcal{D}_a/\partial\omega|_l$ is estimated on neglect of κ to be

$$\left.\frac{\partial \mathcal{D}_a}{\partial \omega}\right|_l \approx -\frac{2\omega_l\beta_l^2 D_4}{\omega_0^2} \tag{51}$$

where β_l may be set to be $(k_l^2 - \omega_0^2)^{1/2}$. Hence when κ is small enough, it holds approximately that

$$\frac{\mu_l}{\alpha_l} \approx -\frac{\sigma\kappa\omega_l^3\omega_0^2}{8\nu^2\omega_l'\beta_l^4 D_2^2} \tag{52}$$

Noting that D_4 is the even function of β and that β_l is real or purely imaginary, D_4 is always real. Furthermore because ω_l^3/ω_l' is positive, μ_l/α_l is negative so that no instability occurs around these intersections. Hence the numerical result is endorsed by the asymptotic analysis.

V. Wave Energy and Negative Energy Waves

A. Conservation of Energy

So far we have been concerned only with the dispersion relation and the associated direct instability of the Kelvin–Helmholtz type. Next we consider the stability of wave propagation from a standpoint of the wave energy. Basically, the energy consists of the kinetic and potential energies associated not only with the air in the tunnel, i.e., in the annular region, but also with the beam and the resonators. For their calculation, it is advantageous to work in the moving frame. Taking the velocity potential to be $-U\xi + \Phi(r, \theta, \xi, \tau)$, Eq. (1) is rewritten as

$$\left(\frac{\partial}{\partial\tau} - U\frac{\partial}{\partial\xi}\right)^2 \Phi = a_0^2\left(\frac{\partial^2\Phi}{\partial r^2} + \frac{1}{r}\frac{\partial\Phi}{\partial r} + \frac{1}{r^2}\frac{\partial^2\Phi}{\partial\theta^2} + \frac{\partial^2\Phi}{\partial\xi^2}\right) \tag{53}$$

In terms of Φ, Eq. (2) is given by

$$P(r, \theta, \xi, \tau) = -\rho_0\left(\frac{\partial\Phi}{\partial\tau} - U\frac{\partial\Phi}{\partial\xi}\right) \tag{54}$$

and Eqs. (3) and (10) are rewritten, respectively, as

$$\frac{\partial\Phi}{\partial r} = \left(\frac{\partial H}{\partial\tau} - U\frac{\partial H}{\partial\xi}\right)\cos\theta \qquad \text{at} \qquad r = b \tag{55}$$

and

$$\frac{\partial\Phi}{\partial r} = \frac{V^*}{\rho_0 a_0^2}\left(\frac{\partial P_c}{\partial\tau} - U\frac{\partial P_c}{\partial\xi}\right) \qquad \text{at} \qquad r = R \tag{56}$$

where $P_c(\theta, \xi, \tau) = p_c(\theta, x = \xi + U\tau, t = \tau)$.

Since the wave propagation is in essence one dimensional along the tunnel and all dissipative effects are discarded, we expect the equation for the conservation of energy in the following form:

$$\frac{\partial E}{\partial\tau} + \frac{\partial J}{\partial\xi} = 0 \tag{57}$$

To derive the specific form of E and J, we must start with the respective equations of energy for the air, beam, and cavity. For the air in the tunnel, the conservation of energy is given in the three-dimensional form as follows (see Appendix B):

$$\frac{\partial\varepsilon_a}{\partial\tau} + \nabla\cdot\boldsymbol{j}_a = 0 \tag{58}$$

where ε_a and $\boldsymbol{j}_a$ are defined, respectively, by

$$\varepsilon_a = \frac{\rho_0}{2}\left[\left(\frac{\partial\Phi}{\partial r}\right)^2 + \frac{1}{r^2}\left(\frac{\partial\Phi}{\partial\theta}\right)^2 + \left(\frac{\partial\Phi}{\partial\xi}\right)^2\right] + \frac{P^2}{2\rho_0 a_0^2} - \frac{UP}{a_0^2}\frac{\partial\Phi}{\partial\xi} \tag{59}$$

and

$$\boldsymbol{j}_a = \left(P - \rho_0 U\frac{\partial\Phi}{\partial\xi}\right)\nabla\Phi + \frac{UP}{a_0^2}\frac{\partial\Phi}{\partial\tau}\boldsymbol{e}_\xi \tag{60}$$

with the unit vector $\boldsymbol{e}_\xi$ directed toward the ξ axis. Here the energy density is defined as the difference from the unperturbed state. It is worth noting that the last term in Eq. (59) accounts for the quadratic contribution of the density change P/a_0^2 to the kinetic energy.

The equation of energy for the beam can be derived by multiplying Eq. (4) by $\partial H/\partial\tau$ as follows:

$$\frac{\partial E_b}{\partial\tau} + \frac{\partial J_b}{\partial\xi} = Q_b\frac{\partial H}{\partial\tau} \tag{61}$$

where E_b and J_b are given, respectively, by

$$E_b = \frac{m}{2}\left(\frac{\partial H}{\partial \tau}\right)^2 + \frac{EI}{2}\left(\frac{\partial^2 H}{\partial \xi^2}\right)^2 + \frac{K}{2}H^2 \tag{62}$$

and

$$J_b = EI\left(\frac{\partial H}{\partial \tau}\frac{\partial^3 H}{\partial \xi^3} - \frac{\partial^2 H}{\partial \tau \partial \xi}\frac{\partial^2 H}{\partial \xi^2}\right) \tag{63}$$

The right-hand side of Eq. (61) is the power input by the air. For the resonator, on the other hand, we multiply Eq. (6) by p_c/ρ_0 and Eq. (7) by Bw, respectively, and add them to derive the equation of energy

$$\frac{\partial \varepsilon_c}{\partial t} = Bp_R w \tag{64}$$

where ε_c denotes the kinetic and potential energies involved in a single resonator and is given by

$$\varepsilon_c = \frac{\rho_0}{2}BLw^2 + \frac{Vp_c^2}{2\rho_0 a_0^2} = \frac{V}{2\rho_0 a_0^2}\left[\frac{1}{\omega_0^2}\left(\frac{\partial p_c}{\partial t}\right)^2 + p_c^2\right] \tag{65}$$

Equation (64) equates the power supplied from the tunnel with the rate of increase in ε_c.

With the three equations of energy available, we consider a control volume in the tunnel bounded by the end planes at $\xi = \xi_1$ and $\xi_2 (>\xi_1)$ taken arbitrarily. The lateral surfaces are taken to be the inner and outer cylindrical surfaces at $r = b$ and R, respectively. Integration of Eq. (58) over this volume leads to

$$\frac{\mathrm{d}}{\mathrm{d}\tau}\int_{\xi_1}^{\xi_2}\mathrm{d}\xi\int_0^{2\pi}\mathrm{d}\theta\int_b^R \varepsilon_a r\,\mathrm{d}r + [J_e]_{\xi=\xi_1}^{\xi=\xi_2} + J_i + J_o = 0 \tag{66}$$

where $[\ldots]_{\xi=\xi_1}^{\xi=\xi_2}$ signifies the quantity in the brackets evaluated at $\xi = \xi_2$ minus that at $\xi = \xi_1$ and J_e, J_i and J_o are given, respectively, by

$$J_e = \int_0^{2\pi}\mathrm{d}\theta\int_b^R\left[\left(P - \rho_0 U\frac{\partial \Phi}{\partial \xi}\right)\frac{\partial \Phi}{\partial \xi} + \frac{UP}{a_0^2}\frac{\partial \Phi}{\partial \tau}\right]r\,\mathrm{d}r \tag{67}$$

$$J_i = -\int_{\xi_1}^{\xi_2}\mathrm{d}\xi\int_0^{2\pi}\left(P - \rho_0 U\frac{\partial \Phi}{\partial \xi}\right)\frac{\partial \Phi}{\partial r}\bigg|_{r=b} b\,\mathrm{d}\theta \tag{68}$$

and

$$J_o = \int_{\xi_1}^{\xi_2}\mathrm{d}\xi\int_0^{2\pi}\left(P - \rho_0 U\frac{\partial \Phi}{\partial \xi}\right)\frac{\partial \Phi}{\partial r}\bigg|_{r=R} R\,\mathrm{d}\theta \tag{69}$$

Using Eq. (55), one can rewrite the integrand of J_i as

$$-\left(P - \rho_0 U\frac{\partial \Phi}{\partial \xi}\right)\frac{\partial \Phi}{\partial r}\bigg|_{r=b} = \left[-P\frac{\partial H}{\partial \tau} + \rho_0 U\frac{\partial}{\partial \tau}\right.$$
$$\left.\times\left(H\frac{\partial \Phi}{\partial \xi}\bigg|_{r=b}\right) - \rho_0 U\frac{\partial}{\partial \xi}\left(H\frac{\partial \Phi}{\partial \tau}\bigg|_{r=b}\right)\right]\cos\theta \tag{70}$$

Integrating Eq. (70) with respect to θ, the first term on the right-hand side gives simply $Q_b \partial H/\partial \tau$. With this replaced by Eq. (61), we obtain

$$J_i = \frac{\partial}{\partial \tau}\int_{\xi_1}^{\xi_2}\mathrm{d}\xi\left(\rho_0 UbH\int_0^{2\pi}\frac{\partial \Phi}{\partial \xi}\bigg|_{r=b}\cos\theta\,\mathrm{d}\theta\right) + \frac{\partial}{\partial \tau}$$
$$\times\int_{\xi_1}^{\xi_2} E_b\,\mathrm{d}\xi + \left[J_b - \rho_0 UbH\int_0^{2\pi}\frac{\partial \Phi}{\partial \tau}\bigg|_{r=b}\cos\theta\,\mathrm{d}\theta\right]_{\xi=\xi_1}^{\xi=\xi_2} \tag{71}$$

Here the first term stems from the first-order term $-\rho_0 U\partial\Phi/\partial\xi$ in the excess kinetic energy $\frac{1}{2}\rho_0[(-U + \partial\Phi/\partial\xi)^2 - U^2]$. It vanishes upon integration over the control volume. But because the actual domain of integration extends from $r = b + H\cos\theta$ to R, the quadratic term results from the integration over the narrow interval from $r = b + H\cos\theta$ to b to yield the first term. Equation (71) shows that the energy flux as a result of the coupling with the beam appears in the last term in the square brackets.

To evaluate J_o, it is convenient to work with x and t in the fixed frame rather than ξ and τ. The transformation of variables from one frame to the other is readily made by the following substitutions: $\partial/\partial t = \partial/\partial\tau - U\partial/\partial\xi$ and $\partial/\partial x = \partial/\partial\xi$. By virtue of Eq. (10) together with Eq. (9), and Eqs. (64) and (8), it follows that

$$\left(P - \rho_0 U\frac{\partial \Phi}{\partial \xi}\right)\frac{\partial \Phi}{\partial r}\bigg|_{r=R} = N^*\frac{\partial \varepsilon_c}{\partial t}$$
$$-\frac{UV^*}{\rho_0 a_0^2}\left\{\frac{\partial}{\partial t}\left(\rho_0 p_c\frac{\partial \Phi}{\partial \xi}\bigg|_{r=R} + \frac{p_c}{\omega_0^2}\frac{\partial^2 p_c}{\partial t \partial x}\right)\right.$$
$$\left.+\frac{\partial}{\partial x}\left[\frac{p_c^2}{2} - \frac{1}{2\omega_0^2}\left(\frac{\partial p_c}{\partial t}\right)^2\right]\right\} \tag{72}$$

The first term on the left-hand side represents the power input into the resonators. The second term results from the quadratic transfer of the first-order kinetic energy $-\rho_0 U\partial\Phi/\partial\xi$ by w^* into the resonators. Introducing Eq. (72) into Eq. (69), J_o can be expressed as

$$J_o = \frac{\partial}{\partial \tau}\int_{\xi_1}^{\xi_2} E_c\,\mathrm{d}\xi + [J_c]_{\xi=\xi_1}^{\xi=\xi_2} \tag{73}$$

where E_c and J_c as a result of all resonators on the periphery of the tunnel are defined, respectively, as

$$E_c = N^*\int_0^{2\pi}\varepsilon_c R\,\mathrm{d}\theta$$
$$-\frac{UV^*}{\rho_0 a_0^2}\int_0^{2\pi}\left(\rho_0 p_c\frac{\partial \Phi}{\partial \xi}\bigg|_{r=R} + \frac{p_c}{\omega_0^2}\frac{\partial^2 p_c}{\partial t \partial x}\right)R\,\mathrm{d}\theta \tag{74}$$

and

$$J_c = -UE_c - \frac{UV^*}{\rho_0 a_0^2}\int_0^{2\pi}\left[\frac{p_c^2}{2} - \frac{1}{2\omega_0^2}\left(\frac{\partial p_c}{\partial t}\right)^2\right]R\,\mathrm{d}\theta \tag{75}$$

Substituting J_i and J_o into Eq. (66), we modify the energy density and flux associated with ε_a and J_e, respectively, to incorporate the first and last terms of J_i in Eq. (71) and define E_a and J_a, respectively, by

$$E_a = \int_0^{2\pi}\mathrm{d}\theta\int_b^R \varepsilon_a r\,\mathrm{d}r + \rho_0 UbH\int_0^{2\pi}\frac{\partial \Phi}{\partial \xi}\bigg|_{r=b}\cos\theta\,\mathrm{d}\theta \tag{76}$$

and

$$J_a = J_e - \rho_0 UbH\int_0^{2\pi}\frac{\partial \Phi}{\partial \tau}\bigg|_{r=b}\cos\theta\,\mathrm{d}\theta \tag{77}$$

With such definitions, Eq. (66) can be recast into the form of Eq. (57) integrated over the control volume where E and J are specified, respectively, as

$$E = E_a + E_b + E_c \tag{78}$$

and

$$J = J_a + J_b + J_c \tag{79}$$

B. Mean Energy Density and Flux

Next we consider the averages of E and J over one period of oscillation $T(=2\pi/\omega')$ in the moving frame, which are defined by

$$\mathcal{E} \equiv \frac{1}{T}\int_\tau^{\tau+T} E\,\mathrm{d}\tau \quad \text{and} \quad \mathcal{J} \equiv \frac{1}{T}\int_\tau^{\tau+T} J\,\mathrm{d}\tau \tag{80}$$

Using the solutions in Sec. III, one can calculate $\mathcal{E}$ as

$$\mathcal{E} = 2\omega' \left\{ \frac{\pi\rho_0\omega}{a_0^2} \int_b^R |f|^2 r\,\mathrm{d}r + \left[\frac{1}{\omega}(m\omega' Uk + EIk^4 + K) + \frac{\pi\rho_0 V^*}{a_0^2 R\mathcal{F}_2^2} \frac{\omega^3}{\left(1-\omega^2/\omega_0^2\right)^2} \right] |C|^2 \right\} \tag{81}$$

Here the integral term results from the first term in Eq. (76). Taking the time average over one period, it follows that

$$\frac{1}{T}\int_\tau^{\tau+T} \mathrm{d}\tau \int_0^{2\pi} \mathrm{d}\theta \int_b^R \varepsilon_a r\,\mathrm{d}r = \frac{2\pi\rho_0\omega\omega'}{a_0^2} \int_b^R |f|^2 r\,\mathrm{d}r + \pi\rho_0 \left[R\frac{\mathrm{d}f}{\mathrm{d}r}\bigg|_{r=R} \bar{f}(R) - b\frac{\mathrm{d}f}{\mathrm{d}r}\bigg|_{r=b} \bar{f}(b) \right] \tag{82}$$

where the overbar implies a complex conjugate. On the other hand, $\mathcal{J}$ is calculated as

$$\mathcal{J} = 2\omega' \left\{ \pi\rho_0 \left(k - \frac{U}{a_0^2}\omega\right) \int_b^R |f|^2 r\,\mathrm{d}r + \left[\pi\rho_0 Ub\omega \frac{\mathcal{F}_1}{\mathcal{F}_2} + 2EIk^3 - \frac{\pi\rho_0 UV^*}{a_0^2 R\mathcal{F}_2^2} \frac{\omega^3}{\left(1-\omega^2/\omega_0^2\right)^2} \right] |C|^2 \right\} \tag{83}$$

The integral of f in Eqs. (81) and (83) is evaluated in Appendix C. Using Eq. (C7), one can show that

$$\mathcal{E} = \omega' \frac{\partial \mathcal{D}}{\partial \omega'} |C|^2 \tag{84}$$

and

$$\mathcal{J} = -\omega' \frac{\partial \mathcal{D}}{\partial k} |C|^2 \tag{85}$$

where $\mathcal{D}$ is regarded as $\mathcal{D}(k, \omega')$. To calculate the partial derivative of $\mathcal{D}$, we regard the left-hand side of Eq. (30) as $\tilde{\mathcal{D}}[\beta(k, \omega'), k, \omega']$ $[=\mathcal{D}(k, \omega')]$ to differentiate as

$$\frac{\partial \mathcal{D}}{\partial \omega'} = \frac{\partial \tilde{\mathcal{D}}}{\partial \beta}\frac{\partial \beta}{\partial \omega'} + \frac{\partial \tilde{\mathcal{D}}}{\partial \omega'} = \frac{\partial \mathcal{D}}{\partial \omega} \tag{86}$$

and

$$\frac{\partial \mathcal{D}}{\partial k} = \frac{\partial \tilde{\mathcal{D}}}{\partial \beta}\frac{\partial \beta}{\partial k} + \frac{\partial \tilde{\mathcal{D}}}{\partial k} \tag{87}$$

with

$$\frac{\partial \beta}{\partial \omega'} = -\frac{\omega}{a_0^2 \beta} \quad \text{and} \quad \frac{\partial \beta}{\partial k} = \frac{1}{\beta}\left(k - \frac{U}{a_0^2}\omega\right) \tag{88}$$

In executing the differentiation $\partial\tilde{\mathcal{D}}/\partial\omega'$ and $\partial\tilde{\mathcal{D}}/\partial k$, it is advantageous to make use of the relation (20). From Eqs. (84) and (85), it follows the well-known result[8] that the ratio $\mathcal{J}/\mathcal{E}$ is nothing but the group velocity, i.e., $\mathcal{J}/\mathcal{E} = -(\partial\mathcal{D}/\partial k)/(\partial\mathcal{D}/\partial\omega') = \mathrm{d}\omega'/\mathrm{d}k$.

C. Positive and Negative Energy Waves

Let us calculate $\partial\mathcal{D}/\partial\omega$ of the dispersion relation shown in Figs. 2–4. The signs attached to the curves indicate that of $\partial\mathcal{D}/\partial\omega$. According to Eq. (84), it is found that all modes in Fig. 2 correspond to those of positive energy waves. In Fig. 3 for the case with $G = \kappa = 0$, it is found for $k > k_f$ that the sign in the upper branch is positive, whereas the sign in the lower branch is negative. Denoting by k_s a wave number where the upper branch crosses the k axis, it is revealed that the upper branch turns into the mode of negative energy waves in a very narrow region $k_f < k < k_s$. When the lining is introduced, Fig. 4 shows that the sign of $\partial\mathcal{D}/\partial\omega$ is positive in the upper three branches and negative in the lower three branches. But since the cavity mode intersects the dotted line $\omega = Mk$, say, at $k = k_c$, the mode turns into that of negative energy waves for $k > k_c$. It is found numerically that $\partial\mathcal{D}/\partial\omega'$ tends to diverge as k increases beyond k_c. Thus given C, the negative energy density $\mathcal{E}$ increases infinitely in magnitude. But because the group velocity $\mathrm{d}\omega'/\mathrm{d}k$ tends to $-U$, the energy flux $\mathcal{J}$ takes a positive value and increases infinitely. Finally we remark that when G vanishes but with $\kappa = 0.1$, the qualitative features remain the same as those in Fig. 3 for $\kappa = 0$ and the negative energy waves emerge in $k_f < k < k_s$.

VI. Conclusions

This paper has examined aeroelastic wave propagation in the air-beam-cavity system to examine the stability of a beam traveling in a tunnel lined acoustically with Helmholtz resonators. It is found from the lossless dispersion relation that there exist a number of branches, which are classified into the acoustic, beam, and cavity modes. When the beam is free from the lateral restoring force, the temporal instability occurs in the beam mode for a long wavelength ($k < k_f$) and a low frequency. Beyond k_f, it is also found that the stable mode turns into that of negative energy waves for a narrow region $k_f < k < k_s$. It is emphasized, however, that the resonators do not take part in this instability. For the numerical values plausible in the actual train–tunnel system, the wavelength corresponding to k_f is so long that it may become comparable with a train's whole length. To discuss the stability in this case, it becomes necessary to take account of end effects ignored in this analysis.

When the restoring force is present, all modes become neutrally stable for the present choice of the parameters. Therefore it may be concluded that the lining does not give rise to the direct instability of the Kelvin–Helmholtz type. But it is found that the cavity mode turns into the mode of negative energy waves for a short wavelength ($k > k_c$). This suggests that the cavity mode may be destabilized by weak dissipative effects. In designing the resonators, this point should be taken into account. The natural frequency chosen here ($\omega_0 = 1.25$) corresponds physically to 13.5 Hz, whereas k_c corresponds to the critical wavelength of about 10 m long. This implies that the natural frequency should be chosen higher to avoid the instability since the critical wavelength becomes short in proportion to ω_0. This condition is consistent with another requirement that the natural frequency should be chosen high enough to inhibit emergence of shock waves.

In practice, however, if the wavelength corresponding to k_c will become comparable or shorter than the spacing between the resonators, then the continuum approximation breaks down and the discrete character in the distribution should be taken into account. Another problem in reality is the effect of induced axial flow in the tunnel. Although this has been neglected by assuming the lossless and linear wave motions, it will be a next target of investigations to estimate the magnitude of the induced flow and to examine whether or not it can significantly change the present results.

Appendix A: Induced Mass of the Beam in the Tunnel

Assume the beam is rigid and let it be forced to oscillate harmonically in the y direction with a given angular frequency ω and a given complex amplitude C in the form of $h(t) = C\exp(-i\omega t)$. Formally this is the case in which k is set equal to zero in Eq. (11) and the equations that follow. Then the axial motion of the beam is immaterial. The induced mass m_i of the beam per unit axial length is defined by the ratio of the induced inertia $-q_h$, i.e., the force acting on the beam with its sign reversed, to the acceleration $\mathrm{d}^2h/\mathrm{d}t^2$ as

$$m_i = -\frac{i\pi\rho_0 b\omega f(b)}{\omega^2 C} = -\pi\rho_0 b\frac{\mathcal{F}_1}{\mathcal{F}_2} \tag{A1}$$

where β^2 in $\mathcal{F}_1$ and $\mathcal{F}_2$ is $-\omega^2/a_0^2$. In the dimensionless form, m_i is given in reference to the induced mass $\pi\rho_0 b^2$ in the incompressible fluid extending infinitely by

$$\frac{m_i}{\pi\rho_0 b^2} = -\frac{1}{\nu}\left[\frac{\left(1-\omega^2/\omega_0^2\right)\beta D_3 - \kappa\omega^2 D_1/2}{\left(1-\omega^2/\omega_0^2\right)\beta^2 D_4 - \kappa\omega^2\beta D_2/2} \right] \tag{A2}$$

with $\beta^2 = -\omega^2$. Figure A1 displays the induced mass m_i against the dimensionless frequency ω for $\nu = 0.3$, where the solid and broken

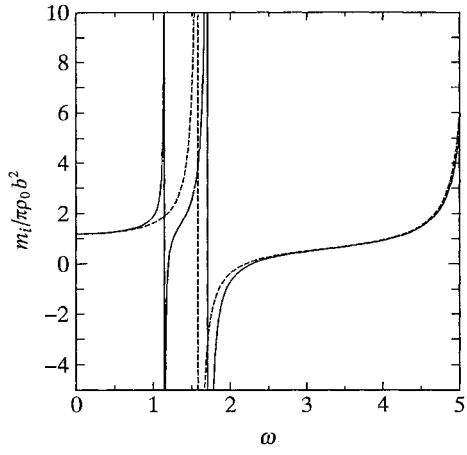

Fig. A1 Graphs of the induced mass m_i of the beam per unit axial length normalized by $\pi\rho_0 b^2$ vs the dimensionless frequency ω for $\nu = 0.3$, where the solid and broken lines represent, respectively, the cases with the lining $\kappa = 0.1$ and $\omega_0 = 1.25$ and without the lining $\kappa = 0$.

lines represent, respectively, the cases with the lining $\kappa = 0.1$ and $\omega_0 = 1.25$ and without the lining $\kappa = 0$. It is found from Eq. (A2) that m_i diverges at frequencies corresponding to the acoustic and cavity modes for $\sigma = 0$ in the long-wavelength limit as $k \to 0$.

In the low-frequency limit as $\omega \to 0$, we have

$$\frac{m_i}{\pi\rho_0 b^2} = \frac{1+\nu^2}{1-\nu^2} \tag{A3}$$

where use has been made of the asymptotic expressions (35).

Appendix B: Conservation of Energy for the Air

In the moving frame with the beam, the equations of continuity and of motions are given, respectively, by

$$\frac{1}{\rho_0 a_0^2}\left(\frac{\partial P}{\partial \tau} - U\frac{\partial P}{\partial \xi}\right) + \nabla\cdot\boldsymbol{V} = 0 \tag{B1}$$

and

$$\rho_0\left(\frac{\partial \boldsymbol{V}}{\partial \tau} - U\frac{\partial \boldsymbol{V}}{\partial \xi}\right) + \nabla P = 0 \tag{B2}$$

with $\boldsymbol{V} = -U\boldsymbol{e}_\xi + \nabla\Phi$ where $\boldsymbol{e}_\xi$ is the unit vector in the ξ direction. Multiplying Eq. (B1) by P and taking the inner product of Eq. (B2) and $\boldsymbol{V}$, respectively, to add them, it follows that

$$\left(\frac{\partial}{\partial \tau} - U\frac{\partial}{\partial \xi}\right)\left(\frac{\rho_0}{2}\boldsymbol{V}\cdot\boldsymbol{V} + \frac{P^2}{\rho_0 a_0^2}\right) + \nabla\cdot(P\boldsymbol{V}) = 0 \tag{B3}$$

To express Eq. (B3) in terms of Φ, we make use of the relation

$$\frac{\partial}{\partial \xi}\left(\frac{\rho_0}{2}\boldsymbol{V}\cdot\boldsymbol{V}\right) = -\rho_0 U\frac{\partial^2\Phi}{\partial\xi^2} + \rho_0\nabla\cdot\left(\frac{\partial\Phi}{\partial\xi}\nabla\Phi\right) - \rho_0\frac{\partial\Phi}{\partial\xi}\Delta\Phi \tag{B4}$$

where Δ denotes the Laplacian. The last term on the right-hand side can further be transformed by using Eq. (54) into

$$-\rho_0\frac{\partial\Phi}{\partial\xi}\Delta\Phi = \frac{1}{a_0^2}\frac{\partial}{\partial\tau}\left(P\frac{\partial\Phi}{\partial\xi}\right) - \frac{1}{2a_0^2}\frac{\partial}{\partial\xi}\left[P\left(\frac{\partial\Phi}{\partial\tau} + U\frac{\partial\Phi}{\partial\xi}\right)\right] \tag{B5}$$

where $\Delta\Phi$ is replaced by the left-hand side of Eq. (53) divided by a_0^2. Introducing Eq. (B4) with Eqs. (B5) and (54) for P into Eq. (B3), we can derive Eq. (58) for the three-dimensional equation of the conservation of energy for the air.

Appendix C: Evaluation of the Integral of $|f|^2$

To evaluate the integral of $|f|^2$, consider the following differential equation complementary to Eq. (17):

$$\frac{d^2 g}{dr^2} + \frac{1}{r}\frac{dg}{dr} - \left(\gamma^2 + \frac{1}{r^2}\right)g = 0 \tag{C1}$$

where $g(r)$ is defined over the interval $b < r < R$ and γ^2 is arbitrary. Let g satisfy the same boundary conditions as Eqs. (14) and (16) for f but in the form of their complex conjugate as follows:

$$\frac{dg}{dr} = i\omega\bar{C} \qquad \text{at} \qquad r = b \tag{C2}$$

and

$$\frac{dg}{dr} = \frac{V^*}{a_0^2}\frac{\omega^2}{\left(1-\omega^2/\omega_0^2\right)}g(R) \qquad \text{at} \qquad r = R \tag{C3}$$

where ω is real. If γ is chosen to be equal to β, g coincides with $\bar{f}$. Multiplying, respectively, Eq. (17) by g and Eq. (C1) by f and subtracting them, we derive after integrating with respect to r from $r = b$ to R

$$\int_b^R fgr\,dr = \frac{1}{\gamma^2-\beta^2}\left[r\left(f\frac{dg}{dr} - g\frac{df}{dr}\right)\right]_{r=b}^{r=R} \tag{C4}$$

When we take the limit $\gamma \to \beta$, the left-hand side approaches the integral of $|f|^2 r$ so that it can be calculated by the right-hand side of Eq. (C4). Thanks to L'Hospital's rule, it is evaluated as

$$\lim_{\gamma\to\beta}\frac{1}{\gamma^2-\beta^2}\left[r\left(f\frac{dg}{dr} - g\frac{df}{dr}\right)\right]_{r=b}^{r=R}$$

$$= \frac{1}{2\beta}\lim_{\gamma\to\beta}\frac{\partial}{\partial\gamma}\left[r\left(f\frac{dg}{dr} - g\frac{df}{dr}\right)\right]_{r=b}^{r=R} \tag{C5}$$

where the differentiation with respect to γ is applied to g only. Substituting Eqs. (14), (16), (C2), and (C3) into (C5), the two terms in the parentheses cancel out at $r = R$ and the first term vanishes at $r = b$ on differentiation with respect to γ. Therefore the right-hand side of Eq. (C5) reduces to

$$\frac{b}{2\beta}\frac{df}{dr}\bigg|_{r=b}\lim_{\gamma\to\beta}\frac{\partial g(b)}{\partial\gamma} \tag{C6}$$

In the limit $\gamma \to \beta$, $g(b)$ approaches the complex conjugate of Eq. (29) where β in $\mathcal{F}_1$ and $\mathcal{F}_2$ is replaced by γ and they are even functions of γ, γ^2 being real for the stable mode. Hence the integral of $|f|^2 r$ is evaluated as

$$\int_b^R |f|^2 r\,dr = \frac{b\omega^2}{2\beta}\frac{\partial}{\partial\beta}\left(\frac{\mathcal{F}_1}{\mathcal{F}_2}\right)|C|^2 \tag{C7}$$

References

[1]Sugimoto, N., "Propagation of Nonlinear Acoustic Waves in a Tunnel with an Array of Helmholtz Resonators," *Journal of Fluid Mechanics*, Vol. 244, 1992, pp. 55–78.

[2]Sugimoto, N., "'Shock-Free Tunnel' for Future High-Speed Trains," *Proceedings of International Conference on Speed-up Technology for Railway and Maglev Vehicles (STECH '93)*, Vol. 2, Japan Society of Mechanical Engineers, Tokyo, 1993, pp. 284–292.

[3]Benjamin, T. B., "The Threefold Classification of Unstable Disturbances in Flexible Surfaces Bounding Inviscid Flows," *Journal of Fluid Mechanics*, Vol. 16, 1963, pp. 436–450.

[4]Landahl, M. T., "On the Stability of a Laminar Incompressible Boundary Layer over a Flexible Surface," *Journal of Fluid Mechanics*, Vol. 13, 1962, pp. 609–632.

[5]Cairns, R. A., "The Role of Negative Energy Waves in Some Instabilities of Parallel Flows," *Journal of Fluid Mechanics*, Vol. 92, 1979, pp. 1–14.

[6]Ostrovskii, L. A., Rybak, S. A., and Tsimring, L. S., "Negative Energy Waves in Hydrodynamics," *Soviet Physics—Uspekhi*, Vol. 29, No. 11, 1986, pp. 1040–1052.

[7]Crighton, D. G., and Oswell, J. E., "Fluid Loading with Mean Flow. I. Response of an Elastic Plate to Localized Excitation," *Philosophical Transactions of the Royal Society of London*, Vol. A 335, 1991, pp. 557–592.

[8]Whitham, G. B., *Linear and Nonlinear Waves*, Wiley-Interscience, New York, 1974, pp. 384–397.